

Proceedings of IAU Symposium 376  
Richard de Grijs, Patricia Whitelock and Marcio Catelan, eds.

## The Cepheid Extragalactic Distance Scale: Past, Present and Future

WENDY L. FREEDMAN<sup>1</sup> AND BARRY F. MADORE<sup>2</sup>

<sup>1</sup>*Dept. of Astronomy & Astrophysics, University of Chicago, 5640 S. Ellis Ave., Chicago, IL 60637, USA and  
Kavli Institute for Cosmological Physics, University of Chicago, 5640 S. Ellis Ave., Chicago, IL 60637, USA*

<sup>2</sup>*Carnegie Observatories, 813 Santa Barbara St., Pasadena CA 91101, USA and  
Dept. of Astronomy & Astrophysics, University of Chicago, 5640 S. Ellis Ave., Chicago, IL 60637, USA*

### ABSTRACT

Cepheids have been the cornerstone of the extragalactic distance scale for a century. With high-quality data, these luminous supergiants exhibit a small dispersion in their Leavitt (period–luminosity) relation, particularly at longer wavelengths, and few methods rival the precision possible with Cepheid distances. In these proceedings, we present an overview of major observational programs pertaining to the Cepheid extragalactic distance scale, its progress and remaining challenges. In addition, we present preliminary new results on Cepheids from the *James Webb Space Telescope (JWST)*. The launch of *JWST* has opened a new chapter in the measurement of extragalactic distances and the Hubble constant. *JWST* offers a resolution three times that of the *Hubble Space Telescope (HST)* with nearly 10 times the sensitivity. It has been suggested that the discrepancy in the value of the Hubble constant based on Cepheids compared to that inferred from measurements of the cosmic microwave background requires new and additional physics beyond the standard cosmological model. *JWST* observations will be critical in reducing remaining systematics in the Cepheid measurements and for confirming if new physics is indeed required. Early *JWST* data for the galaxy, NGC 7250 show a decrease in scatter in the Cepheid Leavitt law by a factor of two relative to existing *HST* data and demonstrate that crowding/blending effects are a significant issue in a galaxy as close as 20 Mpc.

*Keywords:* Cepheids, *HST*, *JWST*, Extragalactic Distance Scale, Hubble constant

### 1. INTRODUCTION

No review of the Cepheid distance scale would be complete without recognition of the contribution by Henrietta Swan Leavitt. Leavitt’s 1908 seminal paper (Leavitt 1908) on variable stars in the Large (LMC) and Small (SMC) Magellanic Clouds established the relationship between the period and luminosity of Cepheids. Subsequently, Leavitt and Pickering (2012) published a period–luminosity relation for 25 Cepheids in the SMC, finding a nearly linear relationship between the logarithm of the luminosity and the logarithm of the period. Leavitt and Pickering recognized that the Magellanic Cloud Cepheids were likely at the same distance from Earth, “... their periods are apparently associated with their actual emission of light, as determined by their mass, density and surface brightness.” These critical insights laid the foundation for the Cepheid distance scale, facilitating the measurement of distances to astronomical objects. Leavitt passed away in 1921, and sadly did not live to see the impact of her pioneering work. In 2008, a meeting was held at Harvard University to commemorate the 100-year anniversary of Leavitt’s Cepheid discovery paper. An outcome of the meeting was the recommendation to name the Cepheid period–luminosity relation the ‘Leavitt Law’ (Freedman & Madore 2010).

Beginning in 1923, Edwin Hubble discovered Cepheids (Hubble 1925a,b, 1926) galaxies M33, M31, and NGC 6822, and estimated the distances to these galaxies employing Leavitt’s period–luminosity relation. These and subsequent measurements culminated in his discovery of the relationship between galaxy distances and their recessional velocities (Hubble 1929), and set the foundation for modern cosmology with its implications for the expansion of the Universe.

Building upon a body of work characterizing the nature of variable stars in Milky Way clusters (Bailey 1902, Joy 1949, Hogg 1955) Baade (Baade 1956, Baade & Swope 1963, 1965) unambiguously established the existence of two populations of Cepheid variables, resulting in a recalibration of Hubble’s magnitude scale by 1.5 mag, or a factor of two in distance.

The next major advance in Cepheid studies came with Wisniewski & Johnson’s (1968) photoelectric *UBVRIJKL* observations of Milky Way Cepheids. Their high-precision photometry exhibited two major characteristics of Cepheid light curves: (1) the decrease in amplitude moving from the ultraviolet to the near-infrared, and (2) the shift in the relative phase of maximum light, also with increasing wavelength.

The 1970s through 1990s saw the ‘factor-of-two’ debate over the value of  $H_0$ . In a series of ten papers entitled “Steps Toward the Hubble Constant”, published between 1974 and 1995, Allan Sandage and Gustav Tammann (2006) presented evidence generally favoring a value of  $H_0 \sim 50 \text{ km s}^{-1} \text{ Mpc}^{-1}$ . In contrast, de Vaucouleurs (1993) carried out his own calibration of the distance scale, finding values closer to  $100 \text{ km s}^{-1} \text{ Mpc}^{-1}$ . An early detailed review of these programs was given by Hodge (1981) Hodge optimistically summarized the controversy: “Eventually, I assume, when sufficiently reliable measurements are possible ... there will be some number, such as  $H_0$ , that everyone will agree on, within some reasonable and understood limits.” It would be another 20 years before the *Hubble Space Telescope* (*HST*) Key Project team (Freedman et al. 2001) measured a value of  $H_0$  to 10% accuracy; a number that has stood the test of time.

The accurate measurement of Cepheid distances remains non-trivial. One of the main challenges is distinguishing Cepheids from fainter stars, both resolved and unresolved, that contribute to the overall background of the host galaxy. Avoiding/minimizing the effects of crowding and confusion is crucial for the successful identification and measurement of Cepheids in galaxies. A second challenge is the correction for the presence of dust, which both scatters and absorbs radiation. Cepheids are relatively young stars that have not had time to diffuse far from the locations where they were formed; hence they are found in the dusty disks of spiral (or irregular) galaxies. Third, the luminosity of a Cepheid may have a dependence on the abundance or metallicity of the star.

## 2. ADVANTAGES OF THE NEAR-INFRARED

The recognition of the applicability of near-infrared observations of Galactic Cepheids to the distance scale did not occur immediately, despite the early near-infrared observations made by Wisniewski & Johnson (1968) The first application was by McGonegal et al. (1982) (see Figure 1, left), who elucidated the advantages of the near-infrared, most specifically the decreased sensitivity to reddening and the decrease in the observed width of the Leavitt law, even with only single-epoch observations. The decrease in the width of the period–luminosity relation is primarily due to the decrease in sensitivity of the infrared surface brightness to the intrinsic temperature width of the instability strip. Near-infrared observations allowed for accurate distance determinations even with single, random-phase observations of Cepheids whose periods had already been measured. These single-phase measurements were comparable in accuracy to complete time-averaged magnitudes derived from many nights of observations obtained at blue wavelengths.

## 3. THE ERA OF CCDS AND INFRARED ARRAYS

With a wide wavelength sensitivity range, spanning from the *B* band ( $0.45 \mu\text{m}$ ) to the *I* band ( $0.8 \mu\text{m}$ ), CCD detectors allowed, for the first time, the possibility of high-resolution, panoramic, digital data for the extragalactic distance scale (Freedman 1984). With CCDs one could perform local sky subtraction and point-spread-function fitting to obtain accurate magnitudes and colors. In addition, CCDs enabled the handling of crowding and confusion errors at the one-square-arcsecond level. Furthermore, the large wavelength coverage of CCDs allowed the explicit and direct determination of reddening, by applying the interstellar extinction law as a function of wavelength, and eliminating the need to rely solely on foreground estimates and/or assuming negligible additional reddening (in the host galaxy), as many earlier studies had done. The approach, introduced by Freedman (1988) for determining total line-of-sight extinctions and true distance moduli of extragalactic Cepheids’ multiwavelength data (e.g., see Figure 1, right) applied to single-epoch observations of Cepheids in IC 1613, M31, M33, and NGC 300, among others. In brief, the method involves determining differential apparent moduli by scaling them with respect to the corresponding LMC period–luminosity relations and assuming that the (observed) variation with inverse wavelength can be attributed to selective absorption.

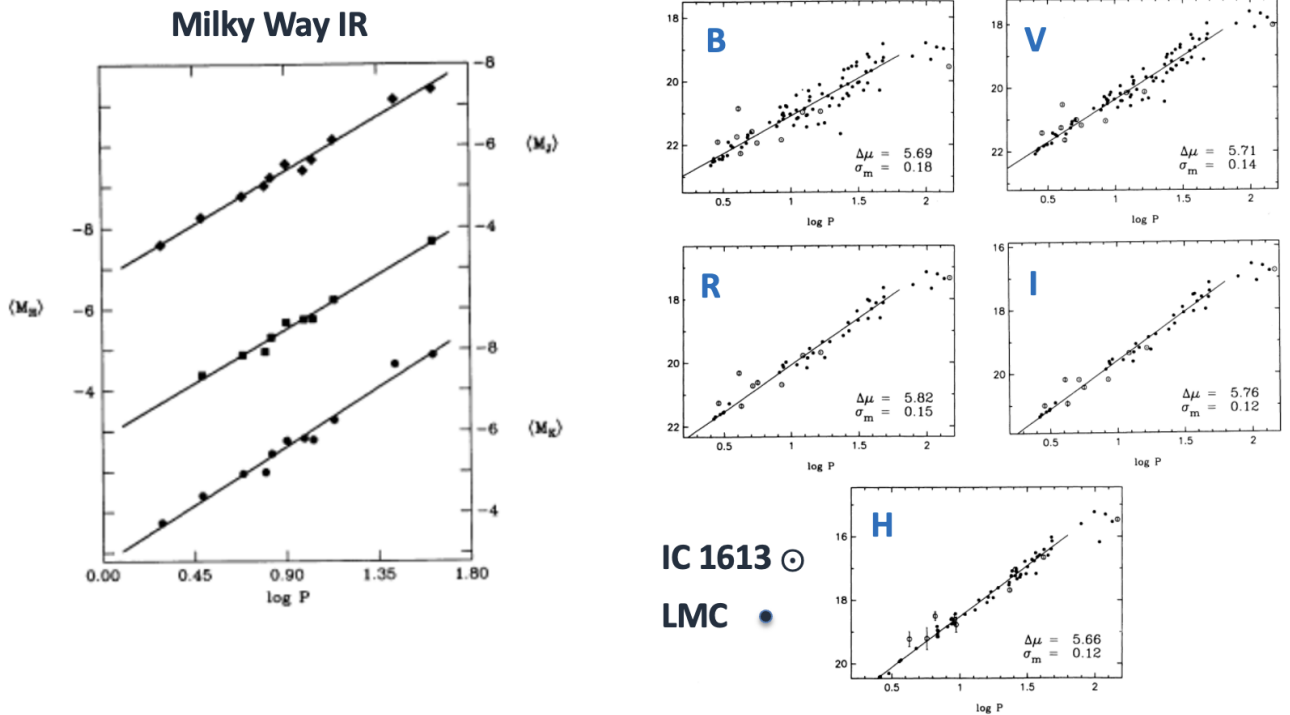


**Figure 1.** Left panel: Leavitt laws at JHK wavelengths (McGonegal et al. 1983) demonstrating the power of infrared photometry for the extragalactic distance scale. Right panel: Leavitt laws at BVRI wavelengths based on CCD photometry (Freedman 1988) (open circles); filled circles illustrate photoelectric photometry for LMC Cepheids.

### 3.1. Metallicity Effects

In addition to reddening, nailing down the metallicity dependence of Cepheids is also critical for application of the Leavitt law. Metallicity can affect the internal structure of a Cepheid: a higher metallicity results in a higher opacity, which can affect the temperature, radius, and luminosity of the star. Line blanketing, controlled by the abundance of metals in the atmospheres of Cepheids, can also result in a redistribution of light as a function of wavelength. The atmospheric effects are predicted to be greater at optical wavelengths than in the infrared.

The availability of CCDs also allowed the first empirical test of metallicity on the Cepheid period–luminosity relation. Freedman & Madore (1990) obtained *BVRI* CCD observations of Cepheids in M31 and estimated the mean reddenings and true distance moduli at three different radial positions (3, 10, and 20 kpc) in the disk of M31, for which a metallicity gradient of a factor of five had been measured from HII regions. They found evidence for a mild gradient of  $-0.2 \pm 0.2$  mag dex $^{-1}$ . However, given the uncertainties, the value was also consistent with no measurable effect.

Twenty-five years later, there still remains uncertainty in the metallicity coefficient Ripepi et al. (2020). A number of recent studies have found a range in the metallicity coefficient from  $-0.5$  to  $0$  mag dex $^{-1}$  (Udalski et al. 2001, Riess et al. 2016, Riess et al. 2021, Breuval et al. 2021, Ripepi et al. 2021, Ripepi et al. 2022). Generally, the effects of metallicity are found to be larger in the optical than in the near-infrared, although in contrast, the recent study by Breuval et al. (2022) finds nearly as large an effect in the near-infrared as in the optical.

## 4. THE HUBBLE SPACE TELESCOPE KEY PROJECT

The goal of the Hubble Key Project (Freedman et al. 2001) was to extend the Cepheid extragalactic distance scale to greater distances than possible from the ground, tie in to several independent methods for measuring distances beyond the Cepheids, and to ultimately measure the Hubble constant to an overall accuracy of 10%. To achieve these goals, the Key Project team used the *HST* to observe Cepheids in 18 galaxies spanning a range of distances. The observations included both wide-field and deep imaging in the F555W and F814W filters, with F555W (*V* band) allowing for the

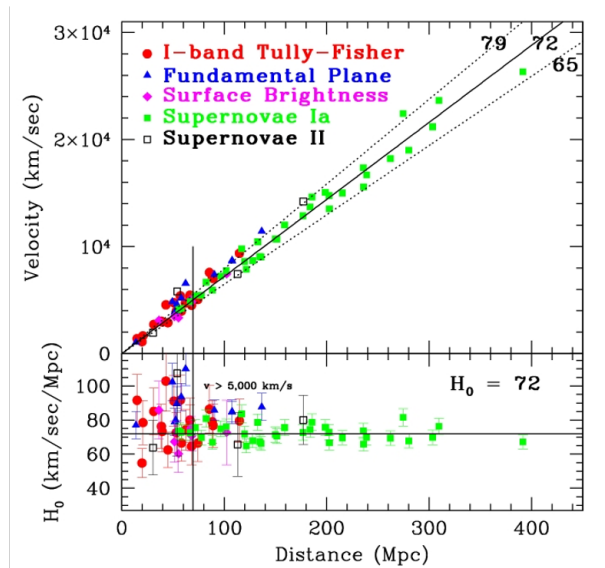


**Figure 2.** Hubble diagram showing the final results from the *HST* Key Project (Freedman et al. 2001) In the top panel velocity is plotted versus distance for the five secondary distance methods labeled in the plot. The solid line is for a slope of 72, flanked by dotted lines indicating a 10% uncertainty. The bottom panel shows the residuals for a value of  $H_0 = 72 \pm 3$  (stat)  $\pm 7$  (sys)  $\text{km s}^{-1} \text{Mpc}^{-1}$ .

discovery, characterization, and measurement of the periods, amplitudes, and mean magnitudes of the Cepheids; and using the longer-wavelength F814W (*I* band) to form a color, thereby providing the means to correct for the effects of extinction and absorption by dust.

These measurements then enabled the calibration of secondary distance indicators (including Type Ia and II supernovae, the Tully–Fisher relation, surface brightness fluctuations, and the  $D_n$ - $\sigma$  relation; see Figure 2). The final value of the Hubble constant was measured as  $H_0 = 72 \pm 3$  (statistical)  $\pm 7$  (systematic)  $\text{km s}^{-1} \text{Mpc}^{-1}$ , with an estimated uncertainty of about 10%. This result provided early evidence for a Universe that is accelerating, consistent with the presence of dark energy, and consistent with the ages of globular clusters. And it resolved the longstanding factor-of-two discrepancy in the distance scale.

## 5. NICMOS AND GROUND-BASED NEAR-INFRARED OBSERVATIONS OF CEPHEIDS

### 5.1. Early NICMOS Observations

Following on the *HST* project, near-infrared observations of 14 nearby galaxies were obtained with *HST*/NICMOS (Macri et al. 2001). Distance moduli were obtained by combining single-epoch *H*-band data with the *VI* bands. These data provided support for the assumption of the universality of the standard (Milky Way) reddening law adopted by the Key Project (see Figure 3), by demonstrating the excellent correspondence between  $E(V - H)$  and  $E(V - I)$ .

An additional goal of the NICMOS program was to undertake another test for the metallicity effect by observing two fields in the relatively face-on galaxy M101, a test that had earlier been undertaken by the Key Project team. The inner and outer M101 fields were found to have a large difference in distance modulus (amounting to  $+0.41 \pm 0.11$  mag at *H* and  $+0.34 \pm 0.09$  mag at *J*, respectively). If interpreted in terms of a metallicity effect, this implies a dependence of order  $0.6 \text{ mag dex}^{-1}$ , much higher than theory predicts for the near-infrared. Simulations, as well as artificial star tests showed that crowding/blending effects were likely an issue for these data, explaining some (but not all) of this large difference.

These results provided a cautionary note regarding the difficulty of measuring Cepheids in the near-infrared in all but the nearest galaxies, and the need to avoid their inner (high-surface-brightness) regions. While the effects of dust are reduced at increasing wavelengths, the background contamination by red stars (red giants and even brighter asymptotic giants) increases substantially. Thus, the advantages of moving to the near-infrared to mitigate extinction effects were countered by the systematic disadvantages imposed by crowding and blending.

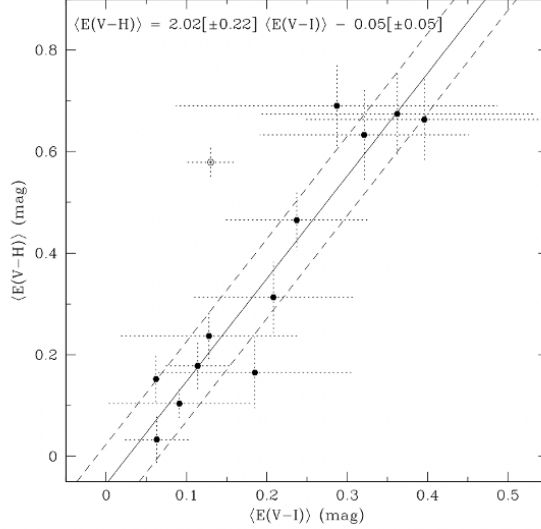


**Figure 3.** A comparison of reddening values measured via  $E(V-H)$  with those from  $E(V-I)$  from Macri et al. (2001). The good agreement provides evidence that a standard extinction law is a reasonable approximation to correct for the dust in these galaxies.

### 5.2. Ground-Based Near-Infrared Observations of the LMC

From the ground, an extensive and uniform near-infrared ( $JHK$ ) study of 92 Cepheids in the LMC was undertaken by Persson et al. (2004), with  $JHK$  sampling obtained at about 22 phase points for each star. The dispersion about the Leavitt law was found to be on the order of  $\pm 0.1$  mag for all three wavebands (see Figure 4). Fitting for a tilt to the LMC, the dispersions in the near-infrared period–luminosity–color relations drop to  $\sim 0.08$  mag, showing again the immense power of the infrared in cases where crowding/blending effects were intentionally minimized and where the signal-to-noise is high. The high quality of these data is apparent when cross-comparing the positions of the individual Cepheids in these period–luminosity relations. The deviations from the mean period–luminosity relations are highly correlated across the various bandpasses, demonstrating intrinsic properties of the Cepheids and/or location within the LMC, that are not blurred out by photometric errors.

## 6. THE SPITZER SPACE TELESCOPE: MID-INFRARED OBSERVATIONS OF CEPHEIDS

Using the IRAC camera on the *Spitzer Space Telescope* during its extended, warm mission, well-sampled mid-infrared light curves were obtained for 80 long-period LMC Cepheids (Scowcroft et al. 2011) falling in the period range  $0.8 < \log(P) < 1.8$  [days]. These observations provided a well-measured slope of the period–luminosity relation based on the time-averaged  $3.6 \mu\text{m}$  data. Time-averaged  $3.6 \mu\text{m}$  data were also obtained for 10 high-metallicity Milky Way Cepheids with independently measured *HST* trigonometric parallaxes (Monson et al. 2012). The  $3.6$  and  $4.5 \mu\text{m}$  Leavitt laws for the LMC can be seen in Figure 4. The  $3.6 \mu\text{m}$  data resulted in a high-precision, reddening-corrected distance to the LMC of  $18.477 \pm 0.033$  (systematic) mag. Freedman et al. (2012) applied the *Spitzer* calibration to the Key Project galaxy sample, yielding a value of  $H_0 = 74.3 \text{ km s}^{-1} \text{ Mpc}^{-1}$ , with a systematic uncertainty of  $\pm 2.1$  (systematic)  $\text{km s}^{-1} \text{ Mpc}^{-1}$ . The *Spitzer* program reduced the systematic uncertainty in  $H_0$  over that obtained by the *Hubble Space Telescope* Key Project by more than a factor of three.

## 7. THE ARAUCARIA PROJECT

For 20 years, the Araucaria Project has been carrying out a program to observe a number of types of variable stars in nearby galaxies at both optical and near-infrared wavelengths (Pietrzynski et al. 2019) They have monitored Cepheid variables, RR Lyrae stars, and eclipsing binaries, as well as blue supergiants, tip of the red-giant branch (TRGB) stars, and carbon stars. The Araucaria Project team has measured Cepheid distances to galaxies in the Local Group (LMC, SMC, IC 1613, NGC 6822, M33), the Sculptor Group (NGC 247, NGC 300, NGC 7793), providing fundamental distances and tests of Cepheid metallicities (Udalski et al. 2001).

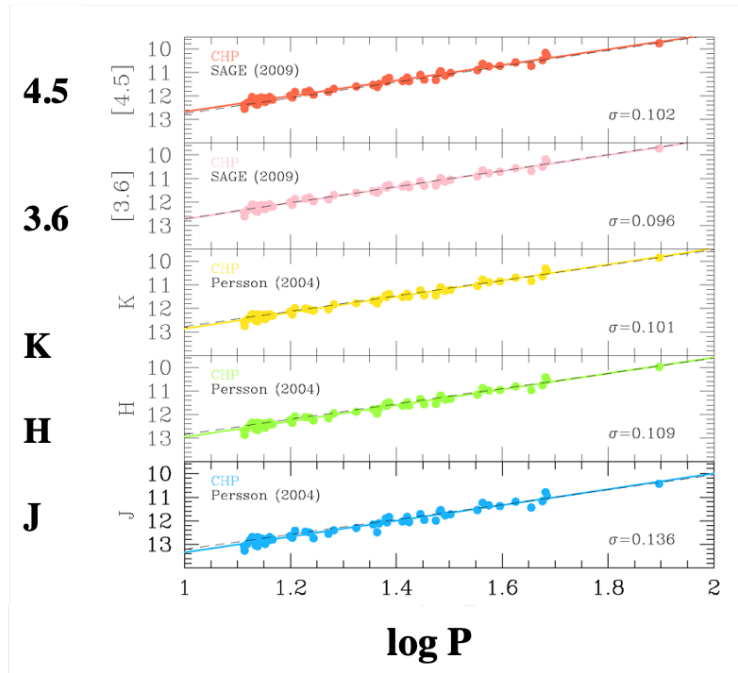


**Figure 4.** Leavitt laws for near-infrared ( $JHK$ ) and mid-infrared ( $3.6$  and  $4.5 \mu\text{m}$ ) for Cepheids in the LMC.

## 8. THE SH0ES PROGRAM

The SH0ES (Supernovae,  $H_0$ , for the Equation of State) project, initially aimed at the study of dark energy, now has the objective of determining  $H_0$  through the calibration of the extragalactic distance scale using Cepheid variables (Riess et al. 2009, 2012, 2016, 2022). Riess and colleagues report *HST* F555W, F814W, and F160W observations of Cepheid variables in host galaxies of Type Ia supernovae (SNe Ia) used to calibrate  $H_0$ . Reddening corrections are obtained using a small number of (2 to 4) random-phase observations in the F814W and F555W bands, with the distances coming mainly from  $\sim 11$  observations taken in the F160W ( $H$ ) band. The scatter in the F160W period–luminosity relations is generally of order 0.4–0.5 mag, i.e., a factor of four or so greater than the intrinsic dispersion observed in the uncrowded sample of Cepheids in the LMC. The zero-point calibration is set by geometric *Gaia* early Data Release 3 (EDR3) parallaxes, masers in the galaxy NGC 4258, and detached eclipsing binaries in the LMC. The most recent SH0ES paper quotes a 1% uncertainty with  $H_0 = 73.04 \pm 1.04 \text{ km s}^{-1} \text{ Mpc}^{-1}$ , based on a sample of 42 galaxies with distances in the range from 7 out to 80 Mpc.

## 9. AN INDEPENDENT EXTERNAL CHECK OF CEPHEID DISTANCES: TIP OF THE RED GIANT BRANCH

Few methods for measuring nearby distances rival the Cepheids in precision, accuracy, or numbers of galaxies for which the measurement can be made. A notable exception is the TRGB method (Lee et al. 1993, Mould & Sakai 2009, Hoyt 2023). The TRGB method also has a number of advantages relative to the Cepheid Leavitt law (Freedman et al 2019, Freedman 2021). It can be applied in the halos of galaxies where the effects of dust are generally negligible and where the surface brightness is about 100 times lower than in the disks, so that crowding/blending effects are not severe. It is a much easier practical issue to measure the luminosity of a halo TRGB star than it is to disentangle Cepheids from nearby neighbors in the disk. In addition, metallicity effects are much smaller for the TRGB (and can be directly calibrated), unlike in the case of Cepheids. Thus, beyond providing an independent calibration of  $H_0$  (Freedman et al. 2019), the TRGB provides an excellent external constraint on the combined systematics of both methods.

In Figure 5 we show a comparison of distance moduli for Cepheids and the TRGB. The agreement between the two distance scales is excellent, with  $\Delta\mu(\text{Cepheid} - \text{TRGB}) = -0.026 \pm 0.014 \text{ mag}$ . In this case, the zero point for the TRGB calibration is  $M_I = -4.05 \text{ mag}$ . The scatter (expectedly) increases with increasing distance and photometric errors.

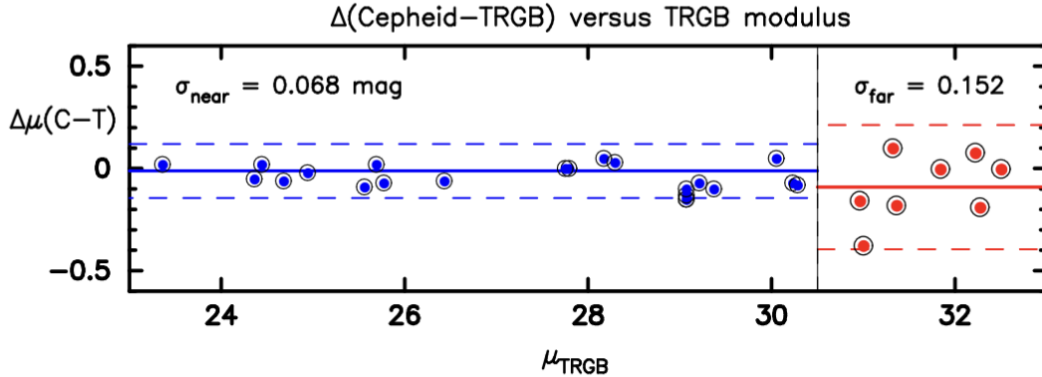


**Figure 5.** Comparison of published Cepheid and TRGB distances in the sense of (Cepheid – TRGB). The blue/red solid lines show the mean offset for galaxies with distance moduli closer/farther than 30.5 mag. The dashed lines indicate the  $1\sigma$  scatter for the near and far samples, which are also labeled in the plot. The agreement between the Cepheid and TRGB distances is excellent, particularly for the nearby sample.

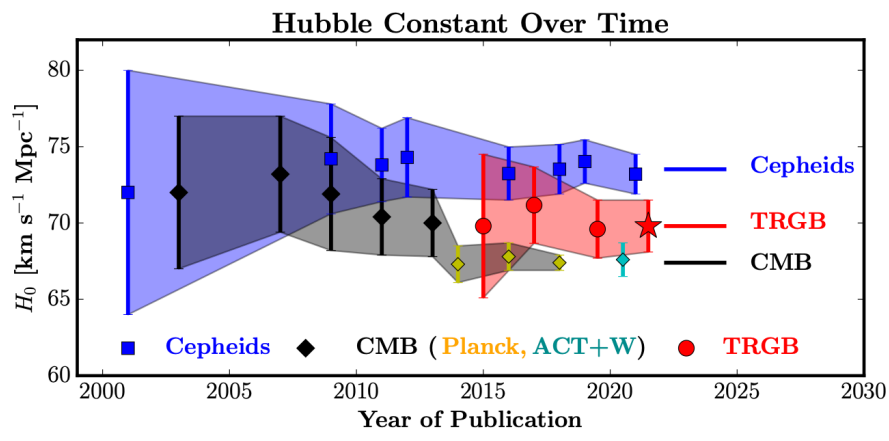


**Figure 6.** Measurements of  $H_0$  from the *HST* Key Project through to today based on Cepheids (blue), the TRGB (red), and the CMB (*Planck*: yellow; ACT + WMAP: turquoise).

In Figure 6 we show an update to a recent comparison of the values of  $H_0$  obtained from Cepheids (blue) and the TRGB (red); both tied into measurements of SNe Ia (Freedman 2021) and that inferred from observations of the cosmic microwave background (CMB; Planck Collaboration et al. 2020, black). The Cepheid and TRGB  $H_0$  values agree to within  $2\sigma$  of their quoted uncertainties; the TRGB measurements are in better agreement with the CMB value to within  $1\sigma$ .

## 10. REMAINING ISSUES FOR THE CEPHEID DISTANCE SCALE

As previously noted, several challenges are still outstanding in measuring Cepheid distances, resulting from the fact that Cepheids are located in regions of star formation within the disks of galaxies, hence in dusty and crowded regions, particularly in their inner disks. The amount (and even the sign) and the wavelength dependence of the metallicity contributions to Cepheid luminosities, within and between galaxies, has yet to converge (Ripepi et al. 2020, Breuval et al. 2021, da Silva et al. 2022, Owens et al. 2023).

Both the *HST* Key Project and the SH0ES group approach the issue of crowding/blending of Cepheids with the use of artificial star tests. Figure 7 (courtesy of I. Jang) shows the F160W crowding-induced bias found for Cepheids observed in nine of the closest SNe Ia host galaxies (Riess et al. 2011). As can be seen, the bias can be quite large,

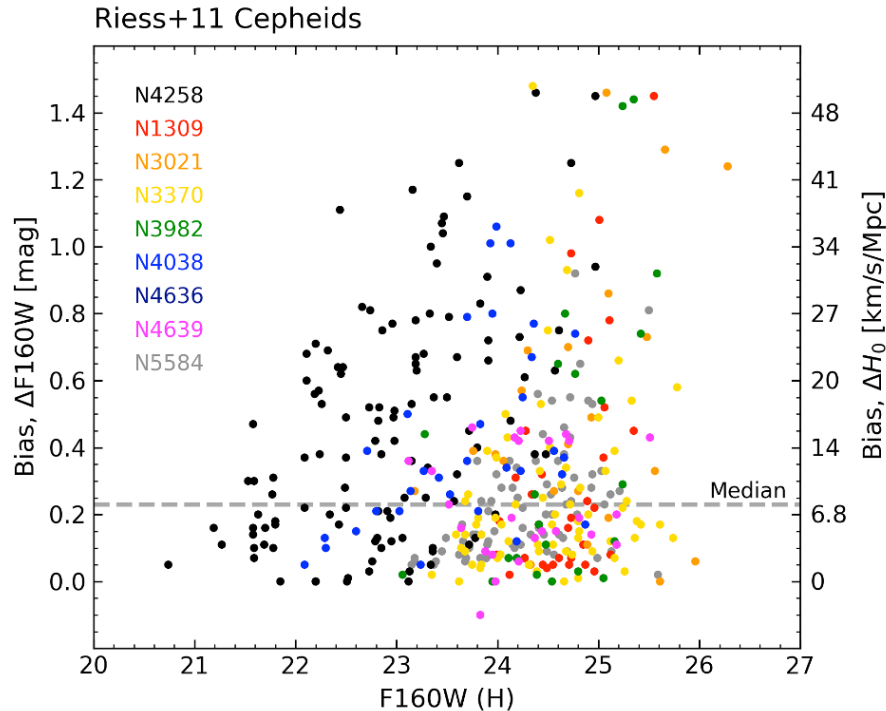


**Figure 7.** A measure of the bias in Cepheid photometry from Table 2 as published by Riess et al. (2011). The bias is determined from artificial star tests for each Cepheid’s environment and is a statistical correction. The bias can be quite significant and ranges from 0 to 1.5 mag (a factor of up to four in luminosity). The median bias is 0.24 mag, corresponding to  $\Delta H_0 = 7 \text{ km s}^{-1} \text{ Mpc}^{-1}$ . The galaxies in this earlier study are amongst the closest in the more recent sample of 42 galaxies in the Riess et al. (2022).

reaching over 1 mag, with a median correction of  $\sim 0.25$  mag, which corresponds to a 10% difference in  $H_0$  of  $> 7 \text{ km s}^{-1} \text{ Mpc}^{-1}$  (as shown to the right of the plot). With the (unexplained) scatter in the F160W period–luminosity relation being as large as 0.4–0.5 mag, accurate crowding corrections are critical. And within that scatter, there remains the potential for a hidden systematic effect that may be difficult to identify and account for.

It is important to note that on average, for similar types of galaxies, crowding effects will become more severe with increasing distance. Sixty percent of the Riess et al. (2022) sample of galaxies in which Cepheids have been discovered lie at greater distances than 20 Mpc, and 25% of the total sample lies beyond 40 Mpc. At a distance of 40 Mpc, four times the area will be contained within a given pixel. For the most distant SH0ES galaxy at 80 Mpc, 16 times the area will be covered. As the need for percent-level accuracy has grown in importance, and given the level of crowding for Cepheids in a galaxy at a distance of only 20 Mpc (see the *JWST* observations in the following section), it remains important to demonstrate that crowding effects do not produce a systematic bias in the photometry and, hence, the distance measurements for these more distant galaxies observed with *HST*.

## 11. THE FUTURE: CEPHEIDS AND JWST

While measurements of the Cepheid distance scale have improved since the time of the Key Project, great strides have been made in measurements of fluctuations in the temperature and polarization of the microwave background (Planck Collaboration 2018). The current controversy over the value of  $H_0$  now requires pushing the determination of local values to limits approaching 1% accuracy, in order to be of comparable accuracy to the CMB measurements. As we have seen, systematic errors have played, and continue to play, a dominant role, keeping more accurate measurement of  $H_0$  a challenge.

Much like the 1970s and 1980s, when local distance measurement differences remained at an impasse, it is clear once again that improvements in technology will be required to settle the current differences, at the few-percent level, for the Cepheid extragalactic distance scale. We describe here a new program using the *James Webb Space Telescope* (*JWST*), aimed at addressing the current systematics in the *HST* measurements of Cepheid distances. The program is actually three-pronged and includes also the measurement of distances to nearby galaxies using not only Cepheids,



but also TRGB stars and carbon/JAGB stars. In this review, however, we describe only the Cepheid portion of this program.

Because of the greater sensitivity of the surface brightness to temperature at bluer (optical) wavelengths, the amplitudes of Cepheid variables are larger than at longer wavelengths. Thus, its blue sensitivity and high spatial resolution (compared to the ground) made *HST* an ideal facility for the *discovery* of Cepheid variables (Freedman et al. 2001, Riess et al. 2016).

Two key features now make *JWST* the optimal telescope for addressing the *accuracy* of measurements of  $H_0$ : its red sensitivity and higher spatial resolution (compared to *HST*, and certainly far exceeding the spatial resolution and sensitivity of *Spitzer*). The extinction is significantly lower: for example,  $A_J$  is smaller by a factor of four relative to the visual extinction,  $A_V$  (Cardelli et al. 1989). For the F115W (*J*-band) filter on *JWST*/Near-Infrared Camera (NIRCAM; Rieke et al. 2023), the sampling resolution is four times that of *HST*/Wide-Field Camera 3 (WFC3) F160W (*H* band), with a FWHM of 0.04 arcsec versus 0.15 arcsec. With  $\sim 4\times$  better resolution than *HST*/*WFC3*, crowding effects are reduced by more than an order of magnitude in flux. This is especially important because, in the near-infrared, contamination of the Cepheids by red giant and asymptotic giant branch stars exacerbates crowding effects relative to optical wavelengths.

As part of the Chicago Carnegie Hubble Program (CCHP), we have been awarded time in *JWST* Cycle 1 (JWST-GO-1995: PI W. L. Freedman, Co-PI B. F. Madore) for a program designed to address specifically known systematic effects: extinction and reddening by dust, metallicity effects, and crowding/blending of stellar images. We are obtaining NIRCAM *J*-band data and, simultaneously, F356W (mid-infrared) observations of 10 nearby SNe Ia-host galaxies with known Cepheids. For calibration purposes, we are also observing NGC 4258, a galaxy with a geometric distance derived from the motions of nuclear  $H_2O$  megamasers. In addition to the *JWST* results, our group is undertaking a complete re-analysis (Owens et al. 2023) of the archival optical and near-infrared *HST* data obtained by the SH0ES group (Riess et al. 2016).

Here, we present some preliminary results from our program for the nearby galaxy NGC 7250, host to SN2013DY, located at a distance of about 20 Mpc. Figure 8 illustrates cut-out images of four Cepheids in NGC 7250 from (Owens et al. 2023). Shown are images at F115W (from *JWST*; top panel) and F160W (from *HST*; bottom panel), which illustrate the superb resolution and the power of *JWST*. As can be seen in the *HST* data, many of the Cepheid candidates are crowded by nearby neighbors.

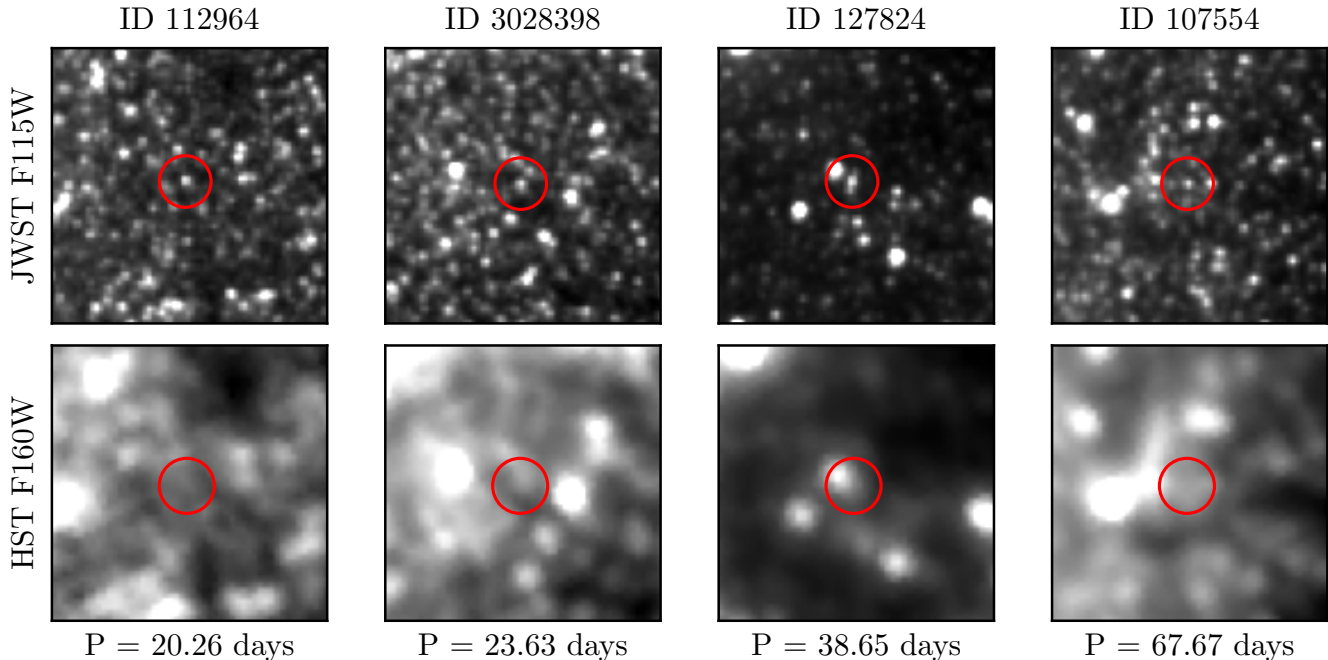


**Figure 8.** Four Cepheids in NGC 7250 discovered as part of the SH0ES project (bottom row: *HST* F160W/*H*-band exposures; top row: *JWST* F115W/*J* band). Each postage-stamp image is  $2 \times 2$  arcsec on a side. The red circles are centered at the position of the Cepheid determined from the *HST* optical (F350LP white light) photometry. It is immediately evident that the crowding for these Cepheids is quite severe and the signal-to-noise ratio (SNR) for the *H*-band data tends to be low, ranging from 1 to 23. In contrast, the SNR for the *J*-band data ranges from 36 to 121. On average, the *JWST* data have almost an order of magnitude greater SNR, and a four times better angular resolution, allowing the Cepheids to be distinguished clearly from the background.

In Figure 9, we show the Leavitt laws for a sample of Cepheids in the LMC (Persson et al. 2004) and in NGC 7250 (Owens et al. 2023). The scatter in the *JWST* F115W data for NGC 7250 is a factor of two smaller than in the SHoES F160W data; i.e., the improved resolution and higher signal-to-noise ratio of the *JWST* data results in a lower variance ( $\sigma^2$ ) for the F115W relation by almost a factor of four. This is all the more remarkable since the *J*-band data are single-phase observations only, while the *HST* observations have been corrected to mean light. The *HST* data exhibit more than three times the scatter of the *H*-band data for the LMC, the latter of which reflects the expected scatter for that band, as exemplified by the LMC data.

## 12. SUMMARY

The accuracy of the Cepheid distance scale has continued to improve over the century during which it has been used to measure the distances to nearby galaxies and set the scale for the determination of  $H_0$ . Still, challenges remain in overcoming systematic uncertainties. Many of these challenges will be overcome with new capabilities provided by the *JWST*.

New *JWST* data for the nearby galaxy NGC 7250 already demonstrate that (1) many of the Cepheids observed with *HST*/*WFC3* are significantly crowded (and biased to brighter apparent magnitudes) by nearby neighbors. A re-analysis of the SH0ES optical data, then coupled with the new high-resolution and higher signal-to-noise *JWST* F115W data, leads to significantly reduced effects of crowding and smaller photometric uncertainties. (2) These improvements result in a factor of two lower scatter in the near-infrared Leavitt law for *JWST* F115W compared with *HST* F160W, even with single-epoch F115W *JWST* photometry.

The galaxies in our *JWST* CCHP program sample have all been selected to have with distances  $\lesssim 20$  Mpc, close enough to minimize crowding effects. As for the case of NGC 7250 presented here, these data will be combined with a re-analysis of the SH0ES *HST* optical data for the Cepheids. TRGB, carbon star, and Cepheid distances to the same sample of galaxies being observed as part of the CCHP will allow measurement of three independent distances to each

## HST and JWST Near-Infrared Cepheid Leavitt Laws

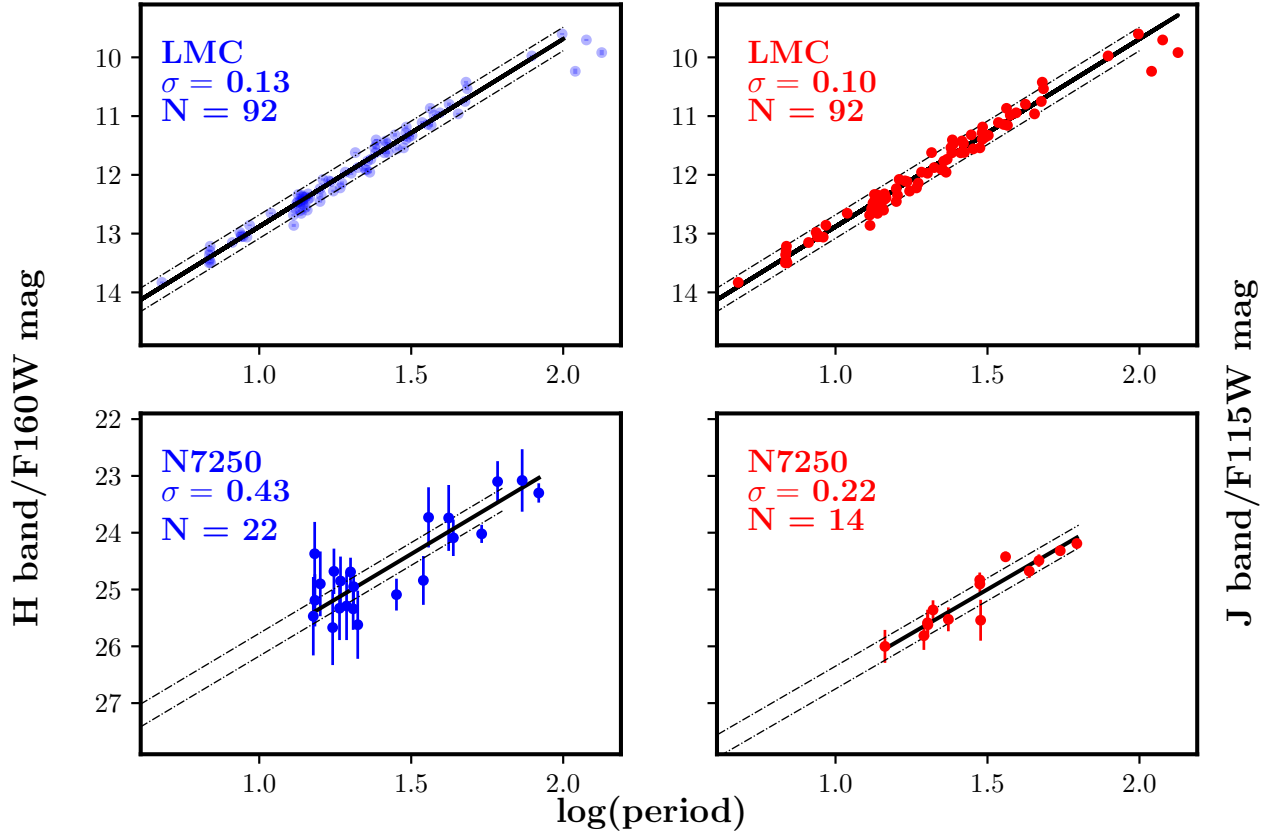


**Figure 9.** Period–luminosity relations for Cepheids in the LMC (top row) and NGC 7250 (bottom row). The left-hand panels are for ground-based  $H$  band for the LMC (top) and the similar F160W filter (from *HST*) for NGC 7250 (bottom). The right-hand panels are similar, but for ground-based  $J$  and the corresponding F115W filter (from *JWST*). The *JWST* data are plotted on an arbitrary magnitude scale. The scatter about the period–luminosity fit in each filter is labeled in each plot.

of these galaxies. These new results already illustrate the power of *JWST* to improve the measurement of extragalactic distances, and specifically, to address remaining systematics in the determination of  $H_0$ .

Ultimately, these data will allow us to provide an answer to one of the most important problems in cosmology today: Is there new fundamental physics required beyond standard  $\Lambda$  Cold Dark Matter?

## REFERENCES

- Baade, W. 1956, *PASP*, 68, 5; doi:10.1086/126870
- Baade, W. & Swope, H. H. 1963, *AJ*, 68, 435; doi:10.1086/108996
- Baade, W. & Swope, H. H. 1965, *AJ*, 70, 212; doi:10.1086/109717
- Bailey, S. I. 1902, *Annals of Harvard College Observatory*, 38, 1
- da Silva, R., Crestani, J., Bono, G., et al. 2022, *A&A*, 661, A104; doi:10.1051/0004-6361/202142957
- Breival, L., Kervella, P., Wielgórski, P., et al. 2021, *ApJ*, 913, 38; doi:10.3847/1538-4357/abf0ae
- Breival, L., Riess, A. G., Kervella, P., et al. 2022, *ApJ*, 939, 89; doi:10.3847/1538-4357/ac97e2
- Cardelli, J. A., Clayton, G. C., & Mathis, J. S. 1989, *ApJ*, 345, 245; doi:10.1086/167900
- de Vaucouleurs, G. 1993, *ApJ*, 415, 10; doi:10.1086/173138
- Freedman, W. L. 1984, *Bull. Am. Astron. Soc.*, 16, 888
- Freedman, W. L. 1988, *ApJ*, 326, 691; doi:10.1086/166128
- Freedman, W. L., Madore, B. F., Gibson, B. K., et al. 2001, *ApJ*, 553, 47; doi:10.1086/320638
- Freedman, W. L., Madore, B. F., Scowcroft, V., et al. 2012, *ApJ*, 758, 24; doi:10.1088/0004-637X/758/1/24
- Freedman, W. L., Madore, B. F., Hatt, D., et al. 2019, *ApJ*, 882, 34; doi:10.3847/1538-4357/ab2f73
- Freedman, W. L. 2021, *ApJ*, 919, 16; doi:10.3847/1538-4357/ac0e95
- Freedman, W. L. & Madore, B. F. 1990, *ApJ*, 365, 186; doi:10.1086/169469
- Freedman, W. L. & Madore, B. F. 2010, *ARA&A*, 48, 673; doi:10.1146/annurev-astro-082708-101829
- Hodge, P. W. 1981, *ARA&A*, 19, 357; doi:10.1146/annurev.aa.19.090181.002041
- Sawyer Hogg, H. 1955, *Publ. David Dunlap Obs.*, 2, 33
- Hoyt, T. J. 2023, *Nat. Astron.*, 7, 590; doi:10.1038/s41550-023-01913-1
- Hubble, E. P. 1925a, *The Observatory*, 48, 139
- Hubble, E. P. 1925b, *ApJ*, 62, 409; doi:10.1086/142943
- Hubble, E. P. 1926, *ApJ*, 63, 236; doi:10.1086/142976
- Hubble, E. 1929, *PNAS*, 15, 168; doi:10.1073/pnas.15.3.168
- Joy, A. H. 1949, *ApJ*, 110, 105; doi:10.1086/145190
- Leavitt, H. S. 1908, *Annals of Harvard College Observatory*, 60, 87
- Leavitt, H. S. & Pickering, E. C. 1912, *Harvard College Obs. Circ.*, 173
- Lee, M. G., Freedman, W. L., & Madore, B. F. 1993, *ApJ*, 417, 553; doi:10.1086/173334
- Macri, L. M., Calzetti, D., Freedman, W. L., et al. 2001, *ApJ*, 549, 721; doi:10.1086/319465
- McGonegal, R., McAlary, C. W., Madore, B. F., et al. 1982, *ApJL*, 257, L33; doi:10.1086/183803
- McGonegal, R., McAlary, C. W., McLaren, R. A., et al. 1983, *ApJ*, 269, 641; doi:10.1086/161071
- Monson, A. J., Freedman, W. L., Madore, B. F., et al. 2012, *ApJ*, 759, 146; doi:10.1088/0004-637X/759/2/146
- Mould, J. & Sakai, S. 2009, *ApJ*, 697, 996; doi:10.1088/0004-637X/697/2/996
- Owens, K., et al. 2023, *ApJ*, submitted
- Persson, S. E., Madore, B. F., Krzemiński, W., et al. 2004, *AJ*, 128, 2239; doi:10.1086/424934
- Pietrzyński, G., Graczyk, D., Gellenne, A., et al. 2019, *Nature*, 567, 200; doi:10.1038/s41586-019-0999-4
- Planck Collaboration, Aghanim, N., Akrami, Y., et al. 2020, *A&A*, 641, A6; doi:10.1051/0004-6361/201833910
- Rieke, M. J., Kelly, D. M., Misselt, K., et al. 2023, *PASP*, 135, 028001; doi:10.1088/1538-3873/acac53
- Riess, A. G., Macri, L., Casertano, S., et al. 2009, *ApJ*, 699, 539; doi:10.1088/0004-637X/699/1/539
- Riess, A. G., Macri, L., Casertano, S., et al. 2012, *ApJ*, 752, 76; doi:10.1088/0004-637X/752/1/76
- Riess, A. G., Macri, L. M., Hoffmann, S. L., et al. 2016, *ApJ*, 826, 56; doi:10.3847/0004-637X/826/1/56
- Riess, A. G., Casertano, S., Yuan, W., et al. 2021, *ApJL*, 908, L6; doi:10.3847/2041-8213/abdbaf
- Riess, A. G., Yuan, W., Macri, L. M., et al. 2022, *ApJL*, 934, L7; doi:10.3847/2041-8213/ac5c5b
- Ripepi, V., Catanzaro, G., Molinaro, R., et al. 2020, *A&A*, 642, A230; doi:10.1051/0004-6361/202038714
- Ripepi, V., Catanzaro, G., Molinaro, R., et al. 2021, *MNRAS*, 508, 4047; doi:10.1093/mnras/stab2460
- Ripepi, V., Catanzaro, G., Clementini, G., et al. 2022, *A&A*, 659, A167; doi:10.1051/0004-6361/202142649
- Sandage, A. & Tammann, G. A. 2006, *ARA&A*, 44, 93; doi:10.1146/annurev.astro.43.072103.150612
- Scowcroft, V., Freedman, W. L., Madore, B. F., et al. 2011, *ApJ*, 743, 76; doi:10.1088/0004-637X/743/1/76
- Udalski, A., Wyrzykowski, L., Pietrzynski, G., et al. 2001, *AcA*, 51, 221
- Wisniewski, W. Z. & Johnson, H. L. 1968, *Commun. Lunar and Planetary Lab.*, 7, 57